



HAL
open science

The effects of single-walled carbon nanotubes (SWCNTs) on the structure and function of human serum albumin (HSA): Molecular docking and molecular dynamics simulation studies

Mehdi Sahihi, Ghazal Borhan

► To cite this version:

Mehdi Sahihi, Ghazal Borhan. The effects of single-walled carbon nanotubes (SWCNTs) on the structure and function of human serum albumin (HSA): Molecular docking and molecular dynamics simulation studies. *Structural Chemistry*, 2017, 28 (6), pp.1815-1822. 10.1007/s11224-017-0963-6 . hal-04086679

HAL Id: hal-04086679

<https://hal.science/hal-04086679>

Submitted on 2 May 2023

HAL is a multi-disciplinary open access archive for the deposit and dissemination of scientific research documents, whether they are published or not. The documents may come from teaching and research institutions in France or abroad, or from public or private research centers.

L'archive ouverte pluridisciplinaire **HAL**, est destinée au dépôt et à la diffusion de documents scientifiques de niveau recherche, publiés ou non, émanant des établissements d'enseignement et de recherche français ou étrangers, des laboratoires publics ou privés.

The effects of single-walled carbon nanotubes (SWCNTs) on the structure and function of human serum albumin (HSA): Molecular docking and molecular dynamics simulation studies

- [Mehdi Sahihi](#) &
- [Ghazal Borhan](#)

Mehdi Sahihi m.sahihi@chem.ui.ac.ir

1 Department of Chemistry, University of Isfahan, Isfahan 81746-73441, Iran

2 Clinical Laboratory, Health Center No. 2, Isfahan University of Medical Science, Isfahan, Iran

Abstract

Here, the interaction of single-walled carbon nanotubes (SWCNTs) and human serum albumin (HSA) as one of the most important proteins for carrying and binding of drugs was investigated and the impact of radius to volume ratio and chirality of the SWCNTs was evaluated using molecular docking method. Molecular docking results represented that zigzag SWCNT with radius to volume ratio equal to $6.77 \times 10^{-3} \text{ \AA}^{-2}$ has the most negative binding energy ($-17.16 \text{ kcal mol}^{-1}$) and binds to the HSA cleft by four π -cation interactions. To study the changes of HSA structure, the complex of HSA-SWCNT was subjected to 30 ns molecular dynamics simulation. The MD results showed that HSA was compressed about 2% after interaction with SWCNT. The equilibrated structure of HSA-SWCNT complex was used to compare the binding of warfarin to HSA in the absence and presence of SWCNT. The obtained results represent that warfarin-binding site was changed in the presence of SWCNT and its binding energy was increased. Really, warfarin was bound on the surface of SWCNT instead of its binding site on HSA. It means that HSA function as a carrier for warfarin is altered, the free concentration of warfarin is changed, and its release is decreased in the presence of SWCNT.

Introduction

Nanotechnology is manipulation of matter on atomic, molecular, and supramolecular scales. A more generalized description of nanotechnology was established by the National Nanotechnology Initiative, which defines nanotechnology as the use of matter with at least one dimension sized from 1 to 100 nm. Nanotechnology is the fourth wave of the industrial revolution, which is developing in all branches of science [1]. Carbon nanotubes (CNTs) have surprising electronic, thermal, optical, structural, and mechanical properties and have received extensive attention in recent years. Their unique geometry makes them appropriate for arrest and transport of gases and liquids. Hence, they have a special role in the medical field, such as drug delivery to target cells [2], biosensors [3], identify and eliminate cancer cells [4], the preparation and transmission of vaccines [5], tissue engineering, and gene transfer and expression [6]. CNTs have high surface area and are potent vehicle for adsorbing or conjugating a wide variety of therapeutic molecules [7]. On the other hand, with the fast progress of the CNTs and their applications, there are rising concerns about the biosafety of these materials to the human health [8,9,10,11]. Porter et al. showed that a CNT can pass a cell membrane and then enter the cytoplasm and nucleus and initiate cell death [12].

Many factors such as length, concentration, type, radius, and functionalization affect the CNT toxicity. Recent studies propose that some features for CNT toxicity are unknown, yet. At a molecular state, interaction of CNT and a biomacromolecule can cause the nanotoxicity. Recently, the interactions of CNTs and proteins are considered by many researchers because of the abovementioned concerns. Proteins are the functional units of life, and their interaction with CNTs can pave the way to answer the basic questions in the nanotoxicology. Park et al. showed experimentally that CNTs can block some membrane ion channels based on their size and shape identity [13]. Insertion of a CNT into the ligand-binding site of a protein can fail the function of affected protein in metabolism pathway of the cell [14, 15]. However, the atomic details of the effect of CNTs on the structure and function of proteins are unclear, due to limitation of the experimental methods [16]. In addition, the dynamics of this interaction is insignificantly understood via experimental methods. Molecular docking and molecular dynamics (MD) simulation are useful methods to investigate the atomic details of the small molecule–protein interactions. Molecular docking and MD simulation are widely used in the studies of biomolecules [17,18,19,20] and nanoscale systems [21,22,23,24,25]. Hence, these computational methods could model the interaction of CNT and protein and avoid some complex side effects.

The mechanism of drug interaction with plasma proteins is key point to understand its pharmacodynamics and pharmacokinetics [26]. Generally, proteins are known as the major targets for most of the drugs in organisms [27]. Their interaction with drug alters the drug absorption, distribution, and elimination in the circulatory system [28] and can prevent its rapid elimination from the blood stream [29]. Human serum albumin (HSA) is the most abundant plasma protein and is known as the dominant transporter plasma protein for endogenous and exogenous ligands (fatty acids, hormones, and drugs) [30]. The HSA binding of a drug can increase its solubility in plasma, decrease its toxicity, protect from oxidation, prolong its in vivo half-life as well as increase the pharmaceutical effect of a drug [31]. Hence, studying the interaction of CNTs with HSA as one of the first targets for binding of these nanomaterials and the effect of CNTs on the structure and function of this carrier protein is essential to understand CNT toxicity.

Here, molecular docking was used to investigate the interaction of various types of SWCNTs (zigzag and armchair) to HSA. Besides, the impact of radius to volume ratio and chirality of the SWCNTs in these interactions was evaluated. Also, the complex of HSA–SWCNT with the most negative standard Gibbs free energy of binding was subjected to MD simulation to study the structural changes of HSA in the presence of SWCNT. Finally, the equilibrated structure of HSA–SWCNT complex was used to compare the binding of warfarin (as a drug which has a high HSA binding affinity and short therapeutic window) to HSA in the absence and presence of SWCNT.

Computational procedures

Molecular docking

All of the docked conformations of SWCNT–HSA complexes were generated through using AutoDock 4.2 molecular docking program [32]. The accuracy of AutoDock 4.2 was checked by redocking the warfarin to HSA. After docking the warfarin back into HSA, the RMSD value between docked warfarin and reference warfarin was 1.9 Å, signifying that AutoDock 4.2 is appropriate for docking of ligands to HSA. Then, docking study was carried out to indicate the HSA-binding site for the selected SWCNTs with various chirality and different radius to volume ratios. The 3D structures of SWCNTs were prepared by VMD software [33], and their structural parameters are given in Table 1. The crystal structure of HSA (PDB ID: 1AO6) was taken from the Brookhaven Protein Data Bank (<http://www.rcsb.org/pdb>). The *R* value and resolution of this

file were 0.218 and 0.25 Å, respectively. It was prepared in pH = 7.5. Water molecules of the protein .pdb file were removed, and missing hydrogen atoms were added. The implemented empirical free energy function and the Lamarckian Genetic Algorithm were used [34]. The Gasteiger charges were added to prepare the macromolecule input file for docking and the Auto Grid was used to calculate Grids. A blind docking with 126 lattice points along X, Y, and Z axes was performed to find the active site of SWCNTs to the HSA. After determination of the active site, the dimensions of the grid map were selected at 60 points with a grid point spacing of 0.375 Å, to allow the SWCNT to rotate freely. Two hundred docking runs with 25,000,000 energy evaluations for each run were performed.

Table 1 Structural parameters of the modeled SWCNTs

Type of SWCNT	(n,m)	Radius to volume ratio (R/V) (Å ⁻²)	Length (nm)	Type of SWCNT	(n,m)	Radius to volume ratio (R/V) (Å ⁻²)	Length (Å)
Zigzag	(3,0)	0.054144	5	Armchair	(2,2)	0.046953	5
	(4,0)	0.040601	5		(3,3)	0.031297	5
	(5,0)	0.032483	5		(4,4)	0.023474	5
	(6,0)	0.027069	5		(5,5)	0.018779	5
	(8,0)	0.0203	5		(6,6)	0.015649	5
	(9,0)	0.018045	5		(4,4)	0.011737	10
	(10,0)	0.016241	5		(6,6)	0.007828	10
	(6,0)	0.013534	10		(7,7)	0.006707	10
	(7,0)	0.0116	10		(8,8)	0.005869	10
	(9,0)	0.009023	10		(7,7)	0.004471	15
(8,0)	0.006767	15	(9,9)	0.003478	15		

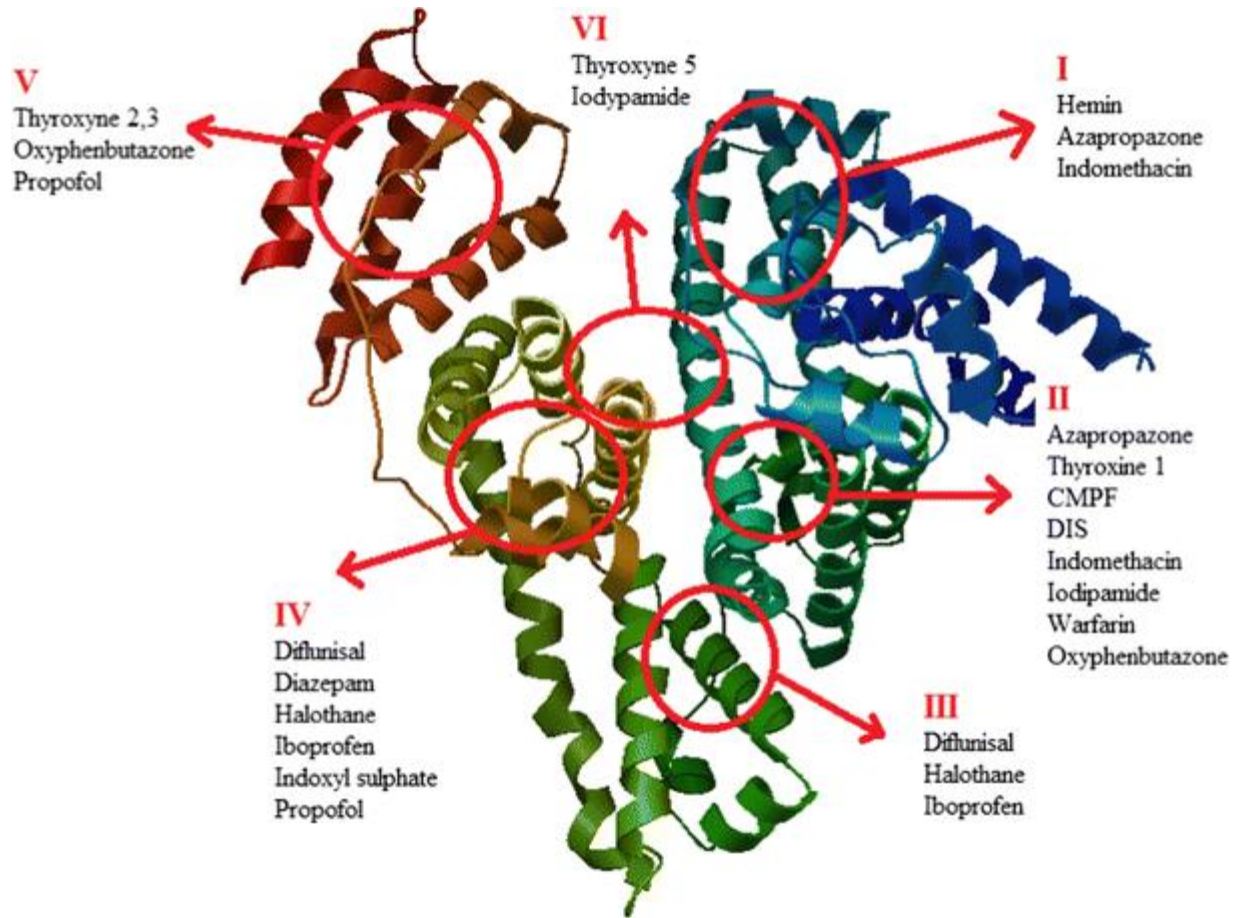
Molecular dynamics (MD) simulation

MD simulation method was used to compare the structural changes of HSA in the absence and presence of SWCNT. The SWCNT–HSA complex with the most negative free-binding energy was considered as the initial conformation for the MD studies. GROMACS 4.6 (University of Groningen, Netherlands) package [35, 36] and OPLS/AA force field [37] were used to carry out all MD studies. The Morse potential and a cosine potential were used to describe the bonds and the angles of the SWCNT. These parameters were used to reproduce experimental results in the CNT–biomolecule system, before [38]. Free protein and SWCNT–HSA complex were located in the cubic box with the periodic boundary conditions in the three directions. The box dimensions were $11.23951 \times 11.23951 \times 11.23951$ nm³ along X, Y, and Z axes, and the minimum distance between protein surface and the box was 1.0 nm. The box was filled with TIP3P water molecules [39], and the solvated system was neutralized by adding 15 sodium ions (Na⁺). After energy minimization using the steepest descent method, the system was equilibrated for 1 ns at the temperature of 300 K. Finally, a 30-ns MD simulation was carried out at 1 bar and 300 K. Parrinello–Rahman barostat [40] at 1 bar, Berendsen thermostat [41] at 300 K, 9 Å cut-off for van der Waals and Coulomb interactions, and the particle mesh Ewald (PME) method [42, 43] for long-range electrostatics were used. The leap-frog algorithm with the 1 fs time step was used to integrate the equation of motions. Finally, an all-bond constrain was used to keep the SWCNT from drifting, and the atomic coordinates were recorded to the trajectory file every 0.5 ps for later analysis. Three independent 30 ns MD simulation per system were performed to probe whole of the phase space.

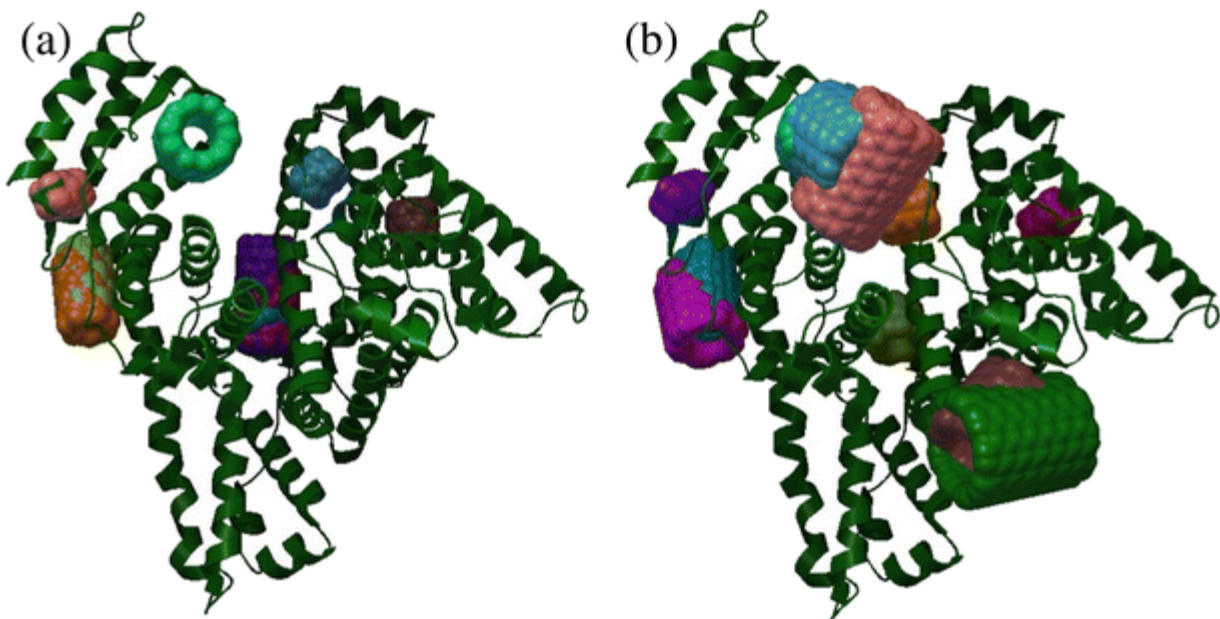
Results and discussion

Molecular docking of SWCNTs to HSA

HSA is a monomeric protein consisting 585 amino acids with I, II, and III α -helical domains. Each domain in HSA is comprised of two subdomains (A and B) [44]. The crystal structure analyses have shown that various drugs are accommodated to one of the six site pockets (Scheme 1) [45]. In the present study, the binding modes of SWCNTs with HSA were examined. The docking results revealed that SWCNTs with various chirality and radius to volume ratios bind in different binding sites of HSA (Fig. 1). Table 2 represents the binding sites and the type of interactions between HSA and each of SWCNTs. Moreover, Fig. S1 represents the binding mode of SWCNTs and shows that hydrophobic, π - π stacking, and π -cation interactions stabilize the SWCNTs in their binding sites. Arginine, lysine, and histidine amino acids as rich electron donor residues and also the carbon of SWCNT have the main roles as π and cation in the π -cation interactions, respectively. Π - π interactions are another type of interactions between SWCNTs and HSA which histidine and phenylalanine play major roles in this type of interaction. The docking energies as function of radius to volume ratio of SWCNTs are presented in Fig. 2. The comparison of binding energies shows that increasing of radius to volume ratio of SWCNTs increases the binding energies of nanotubes to HSA for both zigzag and armchair SWCNTs. By increasing the surface of SWCNT, the probability of its interaction with amino acids in the binding site grows and the docking energy will be raised. The inappropriate dimension of a SWCNT leads to the reduction of interactions and the stability of SWCNT-HSA complex. As can be seen in Fig. 2, the complex of HSA and zigzag (8,0) SWCNT with 15 nm of height has the most negative binding energy. Hence, this CNT has the strongest interaction with HSA, and it can alter the structure and function of HSA with the most probability.



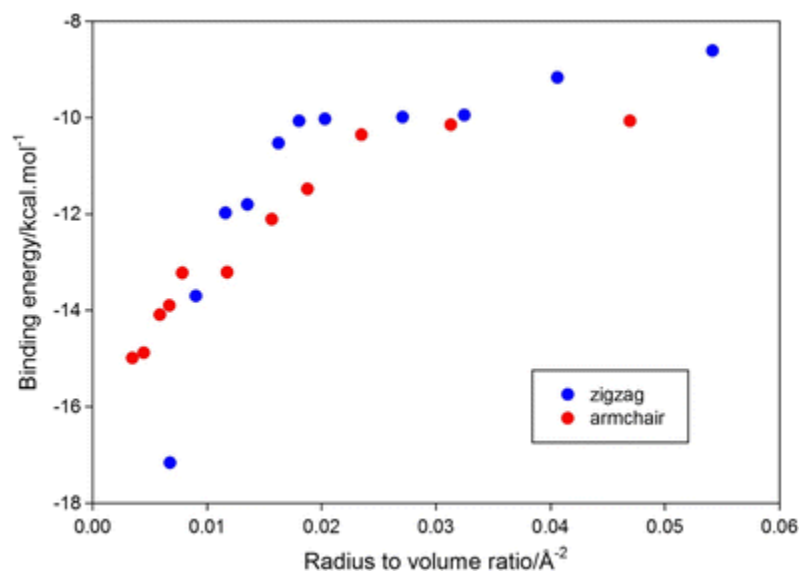
Binding sites of various drugs on HSA



The docking poses of SWCNT–HSA complexes. (a) Zigzag SWCNTs; (b) armchair SWCNTs

Table 2 Molecular docking results for the interaction of SWCNTs with HSA

Type of SWCNT	(n,m)	Height (nm)	Binding site	Type of interactions	Type of SWCNT	(n,m)	Height (nm)	Binding site	Type of interactions
Zigzag	(3,0)	5	V	Hydrophobic	Armchair	(2,2)	5	V	Hydrophobic
	(4,0)	5	V	Hydrophobic, π -cation		(3,3)	5	I	Hydrophobic
	(5,0)	5	I	Hydrophobic		(4,4)	5	I	Hydrophobic, π -cation, π - π
	(6,0)	5	I	Hydrophobic, π -cation		(5,5)	5	VI	Hydrophobic, π -cation
	(8,0)	5	VI	Hydrophobic, π -cation		(6,6)	5	V	Hydrophobic, π -cation
	(9,0)	5	VI	Hydrophobic, π -cation		(4,4)	10	IV	Hydrophobic, π -cation
	(10,0)	5	V	Hydrophobic, π -cation		(6,6)	10	IV	Hydrophobic, π -cation
	(6,0)	10	IV	Hydrophobic, π -cation		(7,7)	10	III	Hydrophobic
	(7,0)	10	IV	Hydrophobic, π -cation		(8,8)	10	V	Hydrophobic
	(9,0)	10	VI	Hydrophobic, π -cation		(7,7)	15	V	Hydrophobic
(8,0)	15	VI	Hydrophobic, π -cation	(9,9)	15	III	Hydrophobic, π - π		



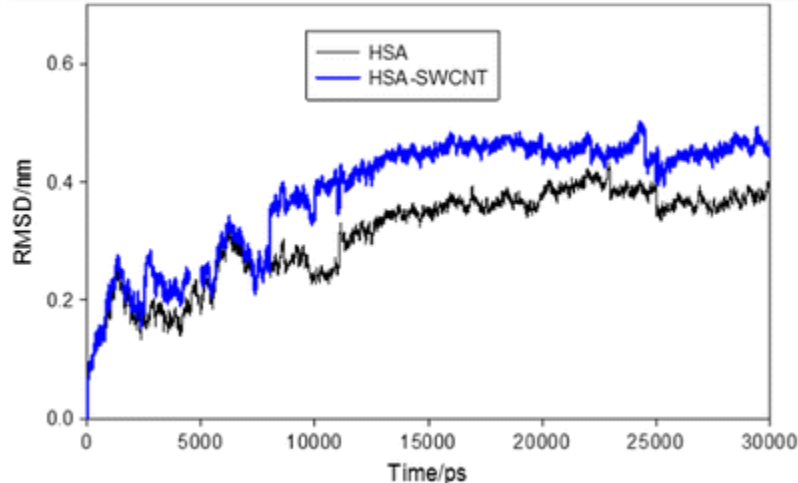
Binding energies of SWCNTs with various radius to volume ratios on HSA

Molecular dynamics simulation

The HSA–SWCNT complex with the most negative binding energy was nominated for MD analysis. The trajectory was analyzed in terms of root mean square deviation (RMSD), radius of gyration (R_g), and root mean square fluctuation (RMSF) using the GROMACS procedures. All of these quantities are mean of three independent 30 ns MD production with periodic boundary condition in all three directions in constant temperature and pressure.

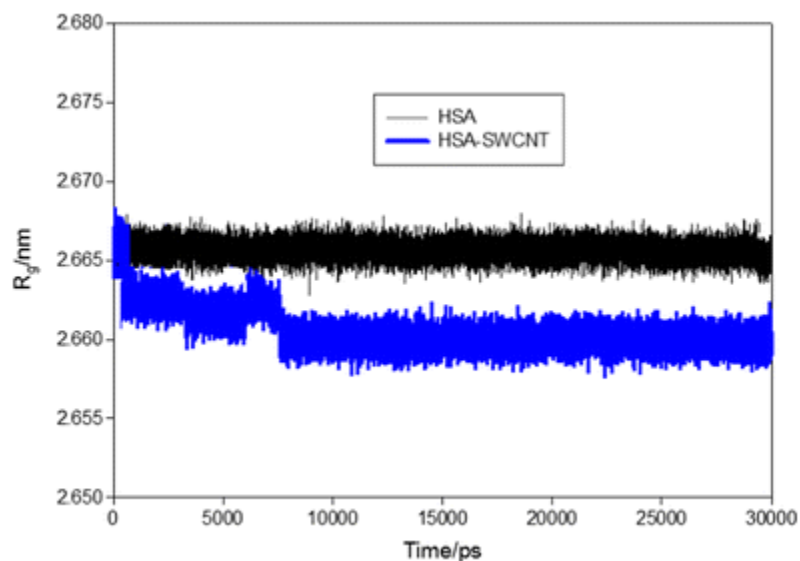
The stability of trajectories for free HSA and HSA–SWCNT complex was studied in terms of RMSD of the backbone of HSA (Fig. 3). Analysis of Fig. 3 shows that the RMSD of free HSA and HSA–SWCNT complex reached equilibrium and fluctuated around their mean values after about 10 ns indicating that these systems were well-behaved thereafter. The RMSD values of free

HSA and HSA–SWCNT complex were calculated from 10 to 30 ns trajectory, where the values were 0.37 ± 0.015 and 0.42 ± 0.011 nm for free HSA and HSA–CNT complex, respectively.



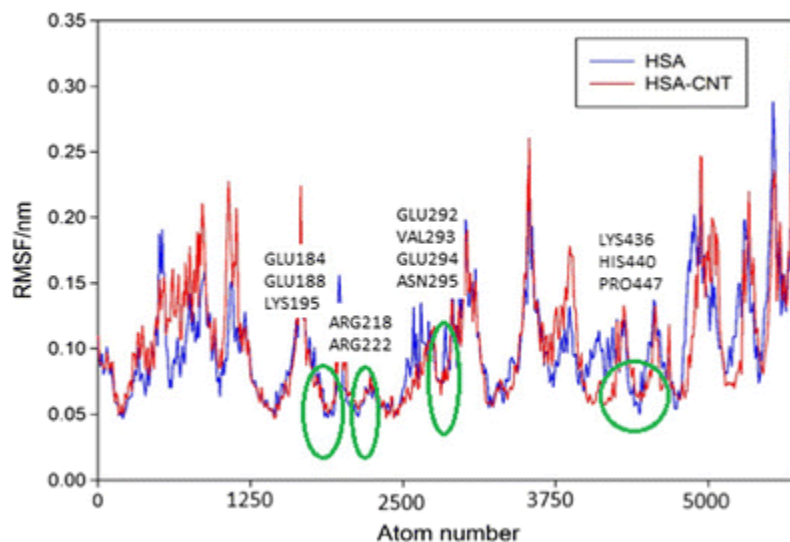
RMSD values for free HSA and HSA–SWCNT complex

The R_g values for the free HSA and HSA–SWCNT complex were also plotted against simulation time to study the protein compactness (Fig. 4). The results showed that the R_g of both systems fluctuates around their mean values after about 7.5 ns, too. The initial R_g values of both system are about 2.7 nm which is in consistent with previous MD simulation study on HSA [46]. The R_g values of free HSA and HSA–SWCNT complex were calculated from a 10–30-ns trajectory, where the values were 2.667 ± 0.001 and 2.660 ± 0.001 nm for free HSA and HSA–SWCNT complex, respectively. The obtained R_g value for HSA is in consistent with the previously reported experimental results [47]. The mentioned results revealed that the radius of gyration value decreased upon complexation of SWCNT with respect to free HSA. Indeed, the SWCNT changes the microenvironment of HSA and the conformation of HSA will be changed during MD simulation. There are same reports that show the HSA conformational changes during the MD simulation for its HSA–fatty acid [48]. As can be seen in Fig. 4, the HSA–SWCNT complex was stabilized around 7.5 ns due to its conformational rearrangement.



Time dependence of R_g during 20 ns of MD simulation

The time-averaged RMSF values were calculated to study the local protein mobility of free HSA and HSA–SWCNT complex. Figure 5 represents the plotted RMSF against atom numbers of protein based on the last 20 ns of trajectory. The profiles of atomic fluctuations for free HSA and HSA–SWCNT complex are similar. The obtained results show that residues participating in binding of SWCNT to protein remain rigid during simulation.

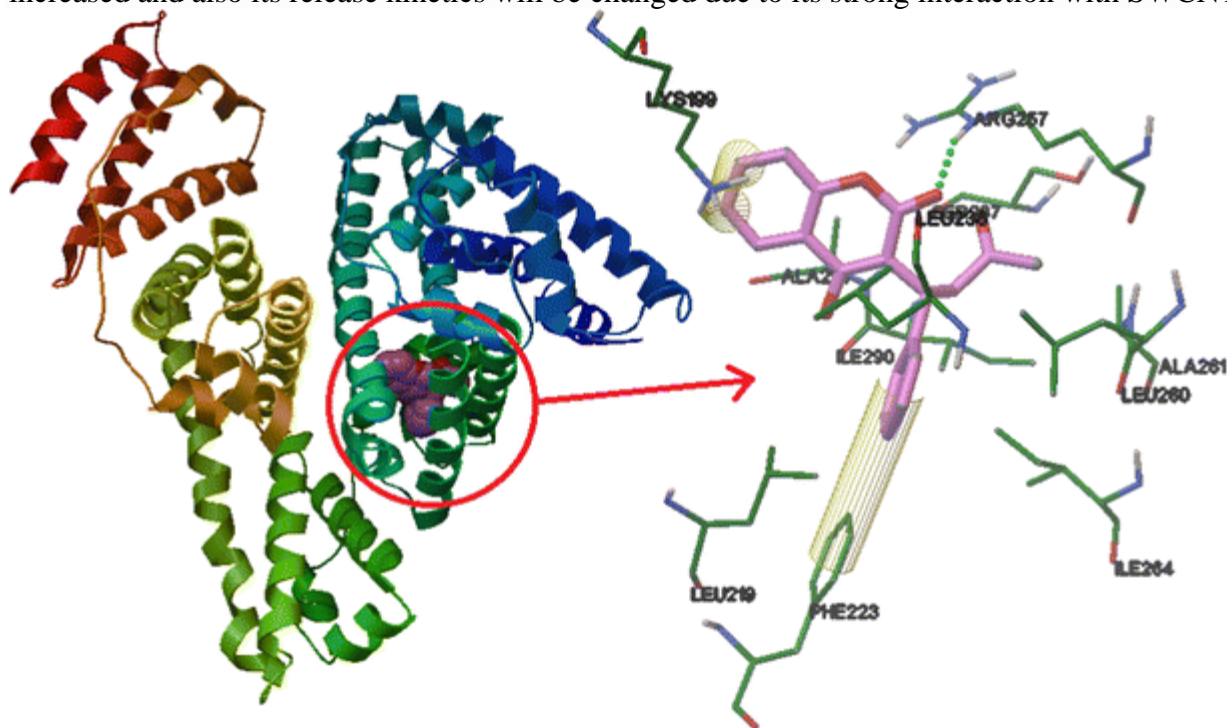


The RMSF values versus atom number of HSA

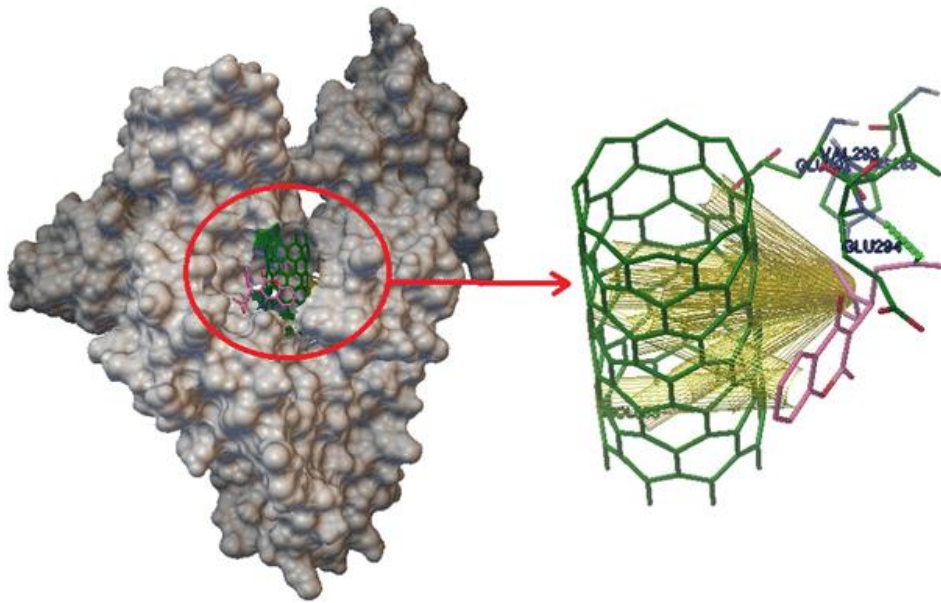
Finally, another MD simulation was ran at 320 K to determine if the results depend significantly on the starting point. The mean values of RMSD and R_g of free HSA and HSA–SWCNT complex at two different temperatures are presented in Table S1. The obtained data show that the results do not depend significantly on the starting point.

Binding of warfarin to the HSA–SWCNT complex

The equilibrated structure of HSA–SWCNT complex after 30 ns of MD simulation was used to compare the binding of warfarin (as a drug which has a high HSA-binding affinity and short therapeutic window) to HSA in the absence and presence of SWCNT. Figure 6 shows the interaction of warfarin within its original binding site on IIA domain of free HSA. However, despite the role of hydrophobic interactions, warfarin binds in this site by one hydrogen bond, two π -cation, and one π - π stacking interactions. The binding energy for HSA–warfarin complex is about $-9.08 \text{ kcal mol}^{-1}$. As it was stated in the previous section, the SWCNT alters the microenvironment of HSA and the conformation of HSA will be changed during MD simulation. This type of structural change may alter the function of HSA as a carrier for a drug with short therapeutic window such as warfarin. To approve or discard this subject, the equilibrated structure of HSA–SWCNT complex was selected as a target for docking of warfarin. Figure 7 represents the binding mode of warfarin to HSA–SWCNT complex. As it is clear from the docking results, warfarin is bound to the surface of SWCNT in the HSA cleft with the docking energy of $-10.93 \text{ kcal mol}^{-1}$. Figure 7 shows that about ten π - π stacking interactions stabilize the warfarin on the surface of SWCNT. Indeed, HSA losses its function as a carrier for warfarin and the drug will be bound to the surface of SWCNT with more negative docking energy than HSA. Hence, the free concentration of warfarin will be decreased and its dosage for the desired effect will be increased and also its release kinetics will be changed due to its strong interaction with SWCNT.



The docking pose of HSA–warfarin complex. Hydrogen bond, π -cation, and π - π stacking interactions represent as *green spheres*, *yellow cone*, and *yellow cylinder*, respectively



The binding mode of warfarin to HSA–SWCNT complex. Hydrogen bond and π – π stacking interactions represent as *green spheres* and *yellow cylinder*, respectively

Conclusions

Here, the interaction of various types of SWCNTs with different radius to volume ratios and HSA was investigated using molecular docking and MD simulation methods to clarify the toxic effects of SWCNT on the structure and function of HSA. The docking results revealed that SWCNTs with various chirality and radius to volume ratios bind in different binding sites of HSA. Moreover, hydrophobic, π – π stacking, and π –cation interactions stabilize SWCNTs in their binding sites. The comparison of binding energies shows that increasing of radius to volume ratio of SWCNTs has direct effect on the interaction of SWCNTs and HSA. The complex of HSA and zigzag (8,0) SWCNT with the height of 15 nm, as the most stable HSA–SWCNT complex, was subjected to 30-ns MD simulation. Analysis of trajectory shows that the RMSD of free HSA and HSA–SWCNT complex reached equilibrium and fluctuated around their mean values after about 10 ns. Also, the MD simulation results revealed that the SWCNT changes the microenvironment of HSA and the conformation of HSA will be changed during MD simulation. Moreover, the profiles of RMSF for free HSA and HSA–SWCNT complex are similar and residues participating in binding of SWCNT to protein remain rigid during simulation. Finally, the equilibrated structure of HSA–SWCNT complex after 30 ns of MD simulation was used to investigate the effect of SWCNT on the function of HSA as a carrier of warfarin. The molecular docking of warfarin to HSA–SWCNT complex revealed that warfarin-binding site will be changed and the drug will be bound to the surface of SWCNT with more negative docking energy than free HSA. Indeed, insertion of SWCNT into the ligand-binding site of HSA can alter the structure of HSA and fail the function of the affected protein.

References

1. Zhao YL, Nalwa HS (2006) Nanotoxicology. American Scientific Publishers, California

2. Bhirde AA, Patel V, Gavard J, Zhang G, Sousa AA, Masedunskas A, Leapman RD, Weigert R, Gutkind JS, Rusling JF (2009) *ACS Nano* 3:307–316
3. Liu N, Zhang Q, Chan-ParkMB, Li C, Chen P (2009) *Nanoscience in biomedicine*. Springer, Germany
4. Thakare VS, Das M, Jain AK, Patil S, Jain S (2010) *Nanomedicine* 5:1277–1301
5. Gorityala B, Ma J, Wang X, Chen P, Liu X (2010) *Chem Soc Rev* 39:2925–2934
6. Zanello LP, Zhao B, Hu H, Haddon RC (2006) *Nano Lett* 6:562–567
7. Bhirde AA, Patel V, Gavard J (2009) *ACS Nano* 3:307–316
8. Gilbert N (2009) *Nature* 460:937–937
9. Donaldson K, Poland CA (2009) *Nat Nanotechnol* 4:708–710
10. Zhao Y, Xing G, Chai Z (2008) *Nat Nanotechnol* 3:191–192
11. Maynard AD, Aitken RJ, Butz T, Colvin V, Donaldson K, Oberdörster G, Philbert MA, Ryan J, Seaton A, Stone V, Tinkle SS, Tran L, Walker NJ, Warheit DB (2006) *Nature* 444:267–269
12. Porter AE, GassM, Muller K, Skepper JN, Midgley PA, WellandM (2007) *Nat Nanotechnol* 2:713–717
13. Park KH, Chhowalla M, Iqbal Z, Sesti F (2003) *J Biol Chem* 278:50212–50216
14. Zuo G, Huang Q, Wei G, Zhou R, Fang H (2010) *ACS Nano* 4:7508–7514
15. Ge C, Du J, Zhao L, Wang L, Liu Y, Li D, Yang Y, Zhou R, Zhao Y, Chai Z (2011) *Proc Natl Acad Sci U S A* 108:16968–16973
16. Shen JW, Wu T, Wang Q, Kang Y (2008) *Biomaterials* 29:3847–3855
17. Mohammadi F, SahihiM, Bordbar AK (2015) *Spectrochim Acta A Mol Biomol Spectrosc* 5:274–282
18. Sahihi M, Ghayeb Y (2014) *Comput Biol Med* 51:44–50
19. Kazemi Z, Amiri-Rudbari H, Sahihi M, Mirkhani V, Moghadam M, Tangestaninejad S, Mohammadpoor-Baltork I, Gharaghani S (2016) *J Photochem Photobiol B Biol* 162:448–462
20. Khosravi I, Hosseini F, KhorshidifardM, Sahihi M, Amiri-Rudbari H (2016) *J Mol Struct* 1119:373–384
21. Gong X, Li J, Lu H, Wan R, Li J, Hu J, Fang H (2007) *Nat Nanotechnol* 2:709–712
22. Hummer G, Rasaiah JC, Noworyta JP (2001) *Nature* 414:188–190
23. Tu Y, Xiu P, Wan R, Hu J, Zhou R, Fang H (2009) *Proc Natl Acad Sci U S A* 106:18120–18124
24. He Z, Zhou J (2014) *Carbon* 78:500–509
25. Giovambattista N, Lopez CF, Rossky PJ, Debenedetti PG (2008) *Proc Natl Acad Sci U S A* 105:2274–2279
26. Cui F, Qin L, Zhang G, Liu Q, Yao X, Lei B (2008) *J Pharm Biomed Anal* 48:1029–1036

27. Lu Y, Cui F, Fan J, Yang Y, Yao X, Li J (2009) *J Lumin* 129:734–740
28. McCallum MM, Pawlak AJ, Shadrack WR, Simeonov A, Jadhav A, Yasgar A, Maloney DJ, Arnold LA (2014) *Anal Bioanal Chem* 406:1867–1875
29. Li F, Feterl M, Warner JM, Day AI, Keene FR, Collins JG (2013) *Dalton Trans* 42:8868–8877
30. Domonkos C, Zsila F, Fitos I, Visy J, Kassai R, Balint B, Kotschy A (2015) *RSC Adv* 5:53809–53818
31. Gou Y, Zhang Y, Qi J, Zhou Z, Yang F, Liang H (2015) *J Inorg Biochem* 144:47–55
32. Morris GM, Huey R, Lindstrom W, Sanner MF, Belew RK, Goodsell DS, Olson AJ (2009) *J Comput Chem* 16:2785–2791
33. Humphrey W, Dalke A, Schulten K (1996) *J Mol Graph* 14:33–38
34. Morris GM, Goodsell DS, Halliday RS, Huey R, Hart WE, Belew RK, Olson AJ (1998) *J Comp Chem* 19:1639–1662
35. Berendsen HJC, Vander Spoel D, Van Drunen R (1995) *Comput Phys Commun* 91:43–56
36. Lindah E, Hess B, Vander Spoel D (2001) *J Mol Model* 7:306–317
37. Jorgensen WL, Maxwell DS, Tirado-Rives J (1996) *J Am Chem Soc* 118:11225–11236
38. Johnson ATC, Staii C, Chen M, Khamis S, Johnson R, Klein ML, Gelperin A (2006) *Semiconduct Sci Technol* 21:S17–S21
39. Jorgensen WL, Chandrasekhar J, Madura JD, Impey RW, Klein ML (1983) *J Chem Phys* 79:926–935
40. Parrinello M, Rahman A (1981) *J Appl Phys* 52:7182–7190
41. Berendsen HJC, Postma JPM, Van Gunsteren WF, DiNola A, Haak JR (1984) *J Chem Phys* 81:3684–3690
42. Darden T, York D, Pedersen L (1993) *J Chem Phys* 98:10089–10093
43. Essmann U, Perera L, Berkowitz ML, Darden T, Lee H, Pedersen LG (1995) *J Chem Phys* 103:8577–8582
44. Carter DC, Ho JX (1994) *Adv Protein Chem* 45:153–203
45. Ghuman J, Zunszain PA, Petitpas I, Bhattacharya AA, Otagiri M, Curry S (2005) *J Mol Biol* 353:38–52
46. Sudhamalla B, Gokara M, Ahalawat N, Amooru DG, Subramanyam R (2010) *J Phys Chem B* 114:9054–9062
47. Kiselev MA, Gryzunov IA, Dobretsov GE, Komarova MN (2001) *Biofizika* 46:423–427
48. Fujiwara S, Amisaki T (2006) *Proteins Struct Funct Bioinf* 64:730–739